ATMOSPHERIC WATER MAPPING WITH THE AIRBORNE VISIBLE/INFRARED IMAGING SPECTROMETER (AVIRIS), MOUNTAIN PASS, CALIFORNIA

James E. Conel, Robert O. Green, Veronique Carrere, Jack S. Margolis, Ronald E. Alley, Gregg Vane, Carol J. Bruegge & Bruce L. Gary

Jet Propulsion Laboratory
California Institute of Technology
Pasadena, California 91109

We report observations of the spatial variation of atmospheric precipitable water using the Airborne Visible/Infrared Imaging Spectrometer (AVIRIS) over a desert area in eastern California, derived using a band ratio method and the 940 nm atmospheric water band and 870 nm continuum radiances. The ratios yield total path water from curves of growth supplied by the LOWTRAN 7 atmospheric model. An independent validation of the AVIRIS-derived column abundance at a point is supplied by a spectral hygrometer calibrated with respect to radiosonde observations. Water values conform to topography and fall off with surface elevation. The edge of the water vapor boundary layer defined by topography is thought to have been recovered. The ratio method yields column abundance estimates of good precision and high spatial resolution.

Atmospheric water vapor is an important reservoir in the global hydrosphere having profound implications for the maintenance of fresh water supplies that are essential for life[1], for energetics of the atmosphere[2] and for modelling the Earth's hydrologic cycle[3] and climate[4]. In addition, water vapor line and continuum absorptions affect quantitative interpretation of the spectral reflectance, which is a fundamental parameter derivable from remote sensing observations of the Earth's surface. We describe here preliminary experiments utilizing spectral radiance band ratios of the Airborne Visible/Infrared Imaging Spectrometer (AVIRIS) that yield high-spatial resolution maps of precipitable atmospheric water. The present band ratio method was modeled after a similar method devised by Farmer *et al.*[5] for measurement of atmospheric water on Mars. The band ratio method offers the possibility of significant improvement in determination of column abundances over mid-infrared and microwave remote sensing techniques. Specification of the time and spatial variability of the absolute amount of water vapor, usually carried out remotely for the terrestrial case by observations at mid-infrared or microwave wavelengths[6] (but see also Ref. 7) contributes to our understanding of surface fluxes through local application of the equation-of-continuity for water vapor. The compensation for water vapor in radiance images of the Earth from aircraft or satellites can be carried out by application of theoretical models of radiative transfer based on molecular absorption line compilations[8,9].

AVIRIS provides near nadir spectral radiance measurements of the Earth from 400-2500 nm[10] with a spectral sampling interval and spectal resolution near 10 nm. From its U-2 platform at an altitude of 20 km above terrain the swath width is 11 km and the surface instantaneous field-of-view (IFOV) 20mx20m. The inflight spectral and radiometric performance of this instrument have been evaluated by field experiment[11]

AVIRIS overflew our test site at Mountain Pass, CA (Lat. 35° 28′ N, Long. 115° 32′ W, Figure 1a) on July 30, 1987, 10:15 AM PST, along a flight line oriented N 55° E. Topographically (Figure 1b) the image area to the northeast contains Ivanpah Valley with Ivanpah Lake (dry) occupying the lowest part at an elevation of 2600 ft (794 m). To the southwest the land surface rises over broad sparsely vegetated alluvial slopes to Clark Mountain and the Mescal Range where the maximum elevation is 6493 ft (1980 m). The image is bordered on the southwest by Shadow Valley at an elevation near 4200 feet (1280 m). During the overflight, measurements were made at site A (elevation 4726 ft., 1441 m)of atmospheric optical depth using a Reagan-type solar radiometer[12] (Figure 2), from which aerosol and ozone optical depths were derived by the procedure of Ref. 13. An observation at wavelength 940 nm was used to derive the slant path precipitable water present by cross-calibration with a ratioing spectral hygrometer (wavelengths 935 nm/880 nm) that is independently calibrated in terms of column precipitable water as determined by about one hundred radiosonde plus high altitude aircraft and large zenith angle solar observations. In addition, the surface bidirectional spectral reflectance of targets within the scene was measured with a portable instantaneous display and analysis spectrometer (PIDAS)[14]. PIDAS covers the spectral range 425-2500 nm with sampling intervals better than 5 nm. Reflectances of uniform areas of Ivanpah Lake (Site B, Figure 1a) were used to generate a local inflight radiometric calibration of AVIRIS[11] through the LOWTRAN 7[8] atmospheric model so that the image digital numbers could be converted to spectral radiance $L(\lambda)$ in $\mu w\ cm^{-2}\ nm^{-1}\ ster^{-1}$. A standard rural aerosol model was employed with visibility of 23 km, adopted by comparison with the Reagan solar radiometer measurements.

Figure 3 is the radiance at AVIRIS spectral resolution predicted at altitude from Ivanpah Lake according to the LOWTRAN 7 standard mid-latitude summer model using the PIDAS-determined surface reflectance as measured at site B. We used the ratio R(940,870,w) of AVIRIS-determined radiances $\overline{L}(940,w)/\overline{L}(870,w)$ (over-bars are averages of three channels around the wavelength indicated and w is precipitable water in cm) to estimate total path precipitable water (downward slant path of zenith angle $\approx$ 29° and upward vertical path) on a point by point basis in the image. The ratios were converted to amounts of water by generating a curve-of-growth from the LOWTRAN 7 model for the altitude of site A, including effects of path radiance intrinsic to the

model for the site altitude and flight conditions. The ratio curve-of-growth has the form $R = Aexp(-B/w)$ where $A = 0.8564$ and, $B = 0.5248$, with correlation coefficient- squared $r^2 = 0.9988$. The total precipitable water calculated from the model for Site A is 3.139 pr. cm. This model neglects the pressure effect from variations in topography over the image away from Site A, which amounts to a few percent.

Figure 1c is a map of the distribution of total precipitable water over the image area. In general atmospheric water distribution conforms to the topography. Notable are differences in amount between Ivanpah Valley and Shadow Valley, which differ in elevation by about 1600 feet (490 m), and a broad area of reduced water abundance found on the topographic slope between Ivanpah Lake and Clark Mountain. Highpoints of the landscape correspond to minimums in observed water abundance. We speculate that the sharp decrease in water column abundance found at the toe of the alluvial slope northeast of Clark Mountain may represent the edge of the water vapor boundary layer. The ratio calculation compensates well for albedo variations (bright and dark areas) over the surface, because the channels used are close to each other in wavelength and the corresponding differences in reflectance are small. The ratio R may be affected by water absorptions in the surface reflectance, either in vegetation or as soil moisture. The presence of an uncompensated surface absorption will decrease the apparent ratio and lead to an apparent increase in atmospheric water calculated to be present. The surface water absorption is always displaced to the red, and any effect of its presence minimized by forming the ratio described above. Also, the sparse desert plant cover present (mainly *Larrea*) and dry climatic conditions probably minimize these effects.

We used the solar radiometer measurements in Figure 2, to estimate precipitable water present at Site A according to the radiosonde-based spectral hygrometer scale, for comparison with the LOWTRAN 7-derived scale. The relationship between solar radiometer ratio $R_{sr} = L(940)/L(870)$ and spectral hygrometer ratio $R_{sr} = L(935)/L(880)$ is $R_{sh} = 0.08703 + 1.07992R_{sr}$ with $r^2 = 0.9999$. The line-of-site precipitable water present is determined from $W_{los} = W_0 + (W_0/6.8)^3$, where $W_0 = 13.7/10^{1.38R_{sh}}$, with an uncertainty ± 10%, including systematic and random errors. The values W_{los} were adjusted for pressure by multiplying by $\sqrt{(p_0/p)}$ where p_0 is sea-level pressure and p is the pressure at site A. The pressure correction factor used is 1.1. Our ratio $R_{sr} = 0.4886$, which yields 2.78 cm of water from the radiosonde scale. This compares favorably with the LOWTRAN 7 value of 3.14 pr cm from the AVIRIS-determined ratio.

The data from separate bands used to generate the ratio image of Figure 1c contain both coherent and random noise components. To improve signal/noise ratio the separate band data were first averaged areally with a 2x2 square filter thereby decreasing the surface spatial resolution by a factor of four.

Horizontal banding present in the ratio image was removed by adjusting the pixels in each line as the difference between the average value for that line and the average value of all pixels in the surrounding ± 25 lines. Periodic microphonic noise was removed by transforming to the Fourier domain, severly attenuating the microphonic noise frequencies, and performing the inverse transform. The random noise component, determined by analysis of single-band imagery over uniform portions of Ivanpah Lake, was found to be ±2% rms. The curve-of-growth yields a fractional uncertainty $\sigma_w/w = 3.8(\sigma_R/R)/\sqrt{w}$ in the determination of w, where σ_R/R is the fractional uncertainty in the ratio, i.e., 4% rms. This gives about ± 0.12 cm of water for average conditions over the Mountain Pass test area.

The present method benefits from a double pass of incident solar radiance through the atmosphere, increasing the observed abundance by approximately $1/\cos\theta$ (θ = solar zenith angle) over the vertical path alone column abundance. The present method offers improvement in precision of retrieved column abundances over that provided by both infrared and microwave remote sounding techniques[15] which have an estimated accuracy of 0.6 - 0.8 pr. cm with present-day instruments. Analysis of sensitivity to effects of scattering and further field validation exercises are planned.

Acknowledgments

We thank Prof. Fred Shair, Caltech, for many useful discussions. This research was carried out at Jet Propulsion Laboratory, California Institute of Technology under contract from the National Aeronautics and Space Administration.

REFERENCES

1. Peixoto, J.P. & Oort, A.H. in *Variations in the Global Water Budget* (eds Street-Perrott, A., Beran, M. & Ratcliffe, R.) 5-65 (Reidel, Dordrecht, 1983).

2. Alestalo, M. in *Variations in the Global Water Budget* (eds Street-Perrott, A., Beran, M. & Ratcliffe, R.) 67-79 (Reidel, Dordrecht, 1983).

3. Brutsaert, W. *Evaporation into the Atmosphere* (Reidel, Dordrecht, 1988).

4. Houghton, J.T. & Morel, P. in *The Global Climate* (ed Houghton, J.T.) 1-11 (Cambridge University Press, Cambridge, 1984).

5. Farmer, C.B., Davies D.W., Holland, A.L., LaPorte, D.D. & Doms, P.E. *J. Geophys. Res.* **82(28)**, 4225-4248 (1977).

6. Houghton, J.T., Taylor, F.W. & Rodgers, C.D. *Remote Sounding of Atmospheres* (Cambridge University Press, Camabridge, 1986).

7. Gorodetsky, A.K. & Syachinov, V.I. in *Variations in the Global Water Budget* (Street-Perrott, A., Meran,M., & Ratcliffe, R.) 81-87 (Reidel, Dordrecht, 1983).

8. Kneizys, F.X., Shettle, E.P., Anderson, G.P., Abrew, L.W., Chetwynd, J.H., Shelby, J.E.A., Clough, S.A., & Gallery W.O. *Atmospheric Transmittance/Radiance: Computer Code LOWTRAN 7* (in press) (1988).

9. Tanre, D., Deroo, C., Duhaut, P., Herman, M., Morcrette, J.J. Perbos, J. & Deschamps, P.Y. in *Proc. Third Int. Colloq. on Spectral Signatures of Objects in Remote Sensing ESA SP* 247 315-319 (1985).

10. Vane, G., Chrisp, M., Enmark, H., Macenka, S., & Solomon, J. *Proc 1984 IEEE Int'l Geoscience and Remote Sensing Symposium ESA SP* 215 751-757 (1984).

11. Conel, J.E., Green, R. O., Alley, R.E., Bruegge, C.J., Carrere, V., Margolis, J., Vane, G., Chrien, T.G., Slater, P.N., Biggar, S.F., Teillet, P.M., Jackson, R.D., & Moran M.S. in *Recent Advances in Sensors, Radiometry, and Data Processing for Remote Sensing SPIE* 924 179-195 (1988).

12. Robinson, B.F., Bauer, M.E., Dewitt, D.P., Silva, L.F. & Vanderbilt, V.C. *SPIE* 196 8-15 (1979).

13. King, D.K. & Byrne, D.M. *J. Atm. Sci.* 33 2242-2251 (1976).

14. Goetz, A.F.H. in *Proceedings of the Third Airborne Imaging Spectrometer Data Analysis Workshop* (ed Vane, G.) *JPL Publication*

87-30 8-17 (1987).

15. Isaacs, R.G., Hoffman, R.N. & Kaplan, L.D. *Rev. Geophys.* 24(4) 701-743 (1986).

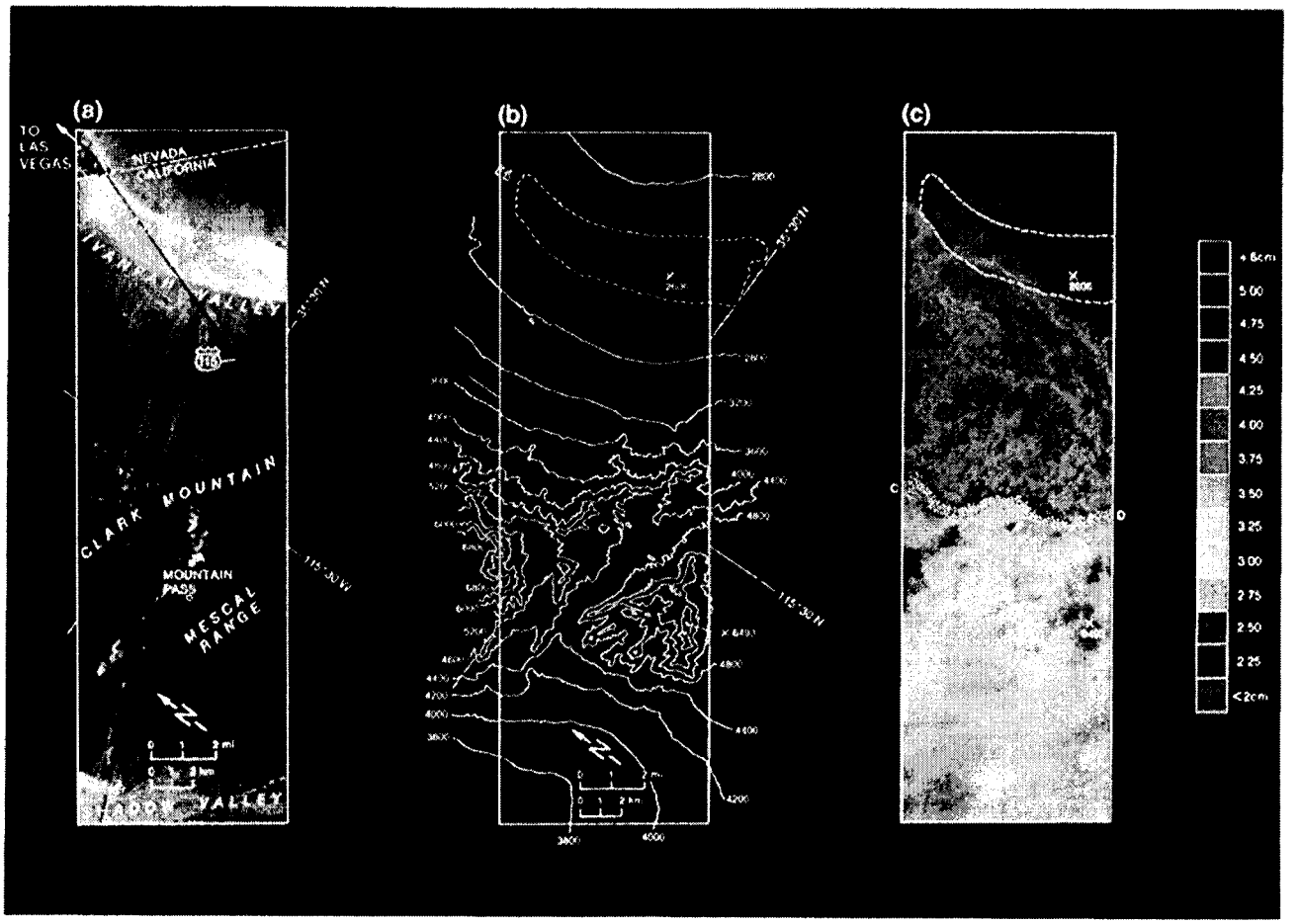

Figure 1. (Refer to slide No. 2.) (a) Three color composite image of the Mountain Pass site using 10 nm channels from AVIRIS, 1537 nm (red), 1051 nm (green), 672 nm (blue). The point (■) labeled A locates station where optical depth was determined; (■) B, a playa target used for inflight calibration of the instrument. (b) generalized topographic map of the site, (c) map of the distribution of precipitable water in cm (color scale at right) determined using the 940 nm atmospheric water band, and the radiance ratio L(940)/ L(870). Stippled region CD marks location of sharp change in mapped water abundance that may represent edge of water vapor boundary layer tapered against the topography.

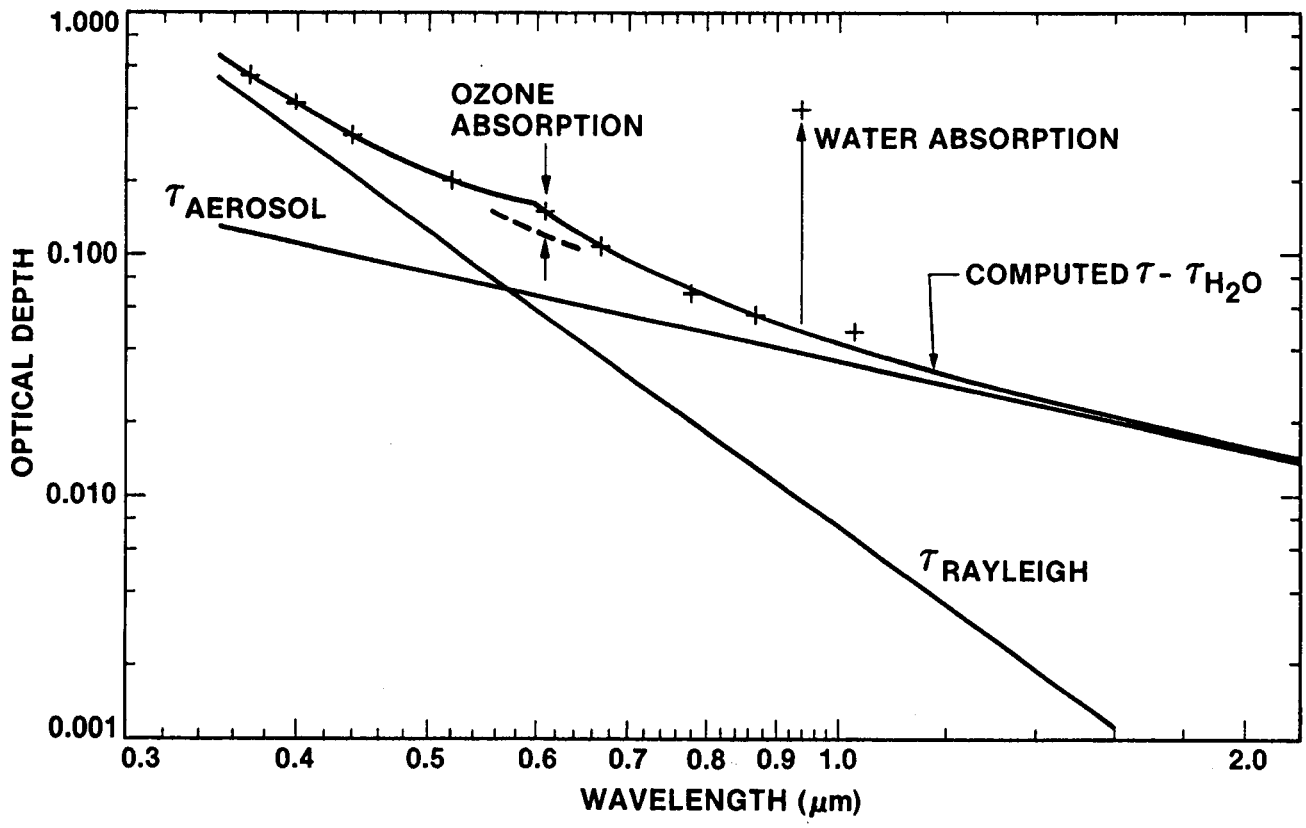

Figure 2. Atmospheric optical depth determined for the clear air conditions of July 30, 1987. (+) are measured points. Rayleigh optical depth $\tau_{RAYLEIGH}$ was computed from the measured atmospheric pressure (856 mb) at time of overflight, 10:15 AM, PST. The line $\tau_{AEROSOL}$ is generated as the best fit to the difference between the observed and Rayleigh optical depths. The ozone optical depth is derived as the difference between observed and sum of Rayleigh and Mie values. The resulting computed optical depth excludes absorption from atmospheric water vapor.

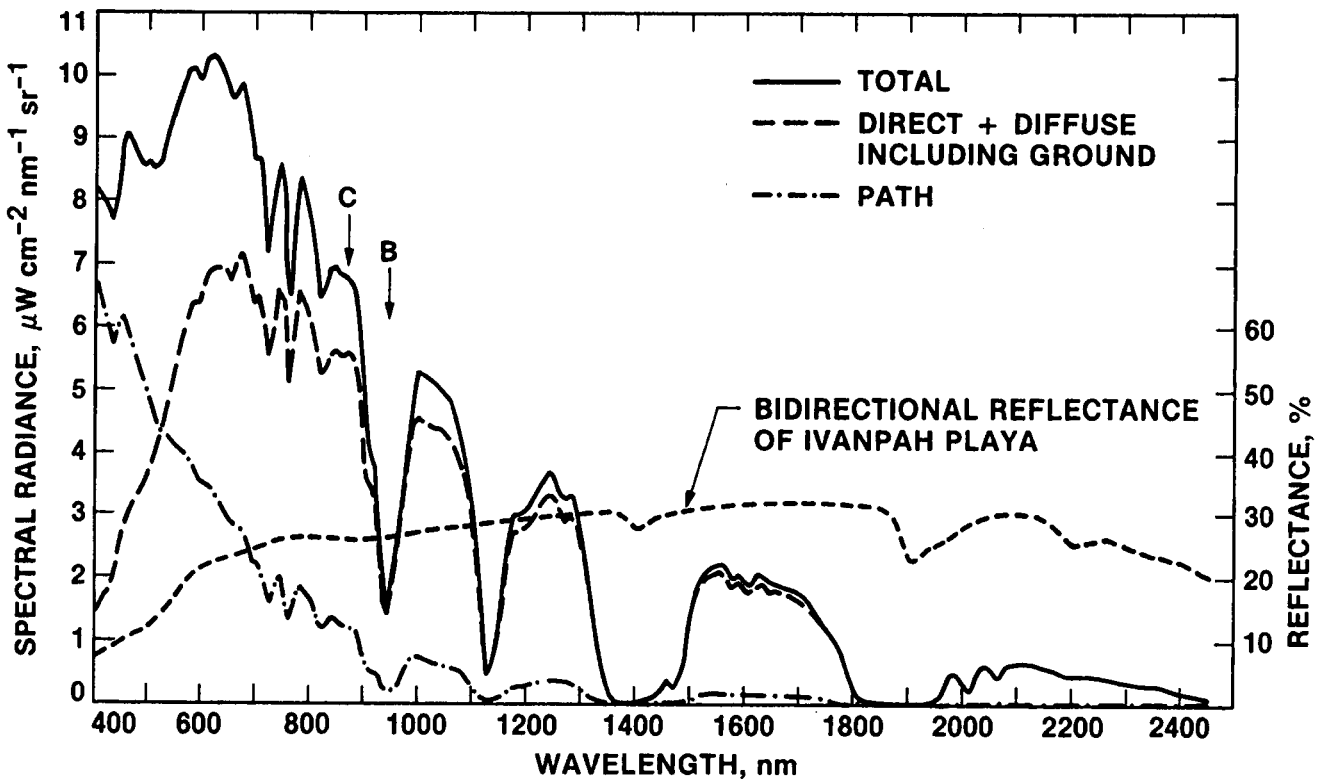

Figure 3. Total radiance, direct plus diffuse ground-reflected radiance, and path radiance generated from LOWTRAN 7 model at AVIRIS observational altitude and spectral resolution over Ivanpah Playa using the spectral reflectance measured at site B (Figure 1a). C and B mark central positions of band clusters used to generate band ratios that are calibrated in terms of atmospheric precipitable water abundances in Figure 1c.